Toxicology in Vitro 80 (2022) 105316

Contents lists available at ScienceDirect

Toxicology in Vitro

journal homepage: www.elsevier.com/locate/toxinvit

The impact of extractable organic matter from gasoline and alternative fuel emissions on bronchial cell models (BEAS-2B, MucilAir™)

Michal Sima [a], Tereza Cervena [a,b], Fatima Elzeinova [a], Antonin Ambroz [a], Vit Beranek [c], Michal Vojtisek-Lom [c], Jiri Klema [d], Miroslav Ciganek [e], Pavel Rossner Jr [a,*]

[a] Department of Nanotoxicology and Molecular Epidemiology, Institute of Experimental Medicine CAS, Videnska 1083, 142 20 Prague, Czech Republic
[b] Department of Physiology, Faculty of Science, Charles University, Vinicna 7, 128 44 Prague, Czech Republic
[c] Centre of Vehicles for Sustainable Mobility, Faculty of Mechanical Engineering, Czech Technical University in Prague, Technicka 4, 160 00 Prague, Czech Republic
[d] Department of Computer Science, Czech Technical University in Prague, 121 35 Prague, Czech Republic
[e] Department of Chemistry and Toxicology, Veterinary Research Institute, 621 00 Brno, Czech Republic

ARTICLE INFO

Editor: Martin Leonard

Keywords:
BEAS-2B
MucilAir™
Extractable organic matter
Exposure
Ethanol blend fuels

ABSTRACT

Air pollution caused by road traffic has an unfavorable impact on the environment and also on human health. It has previously been shown, that complete gasoline emissions lead to toxic effects in cell models originating from human airways. Here we focused on extractable organic matter (EOM) from particulate matter, collected from gasoline emissions from fuels with different ethanol content. We performed cytotoxicity evaluation, quantification of mucin and extracellular reactive oxygen species (ROS) production, DNA breaks detection, and selected gene deregulation analysis, after one and five days of exposure of human bronchial epithelial model (BEAS-2B) and a 3D model of the human airway (MucilAir™). Our data suggest that the longer exposure had more pronounced effects on the parameters of cytotoxicity and mucin production, while the impacts on ROS generation and DNA integrity were limited. In both cell models the expression of *CYP1A1* was induced, regardless of the exposure period or EOM tested. Several other genes, including *FMO2, IL1A,* or *TNF,* were deregulated depending on the exposure time. In conclusion, ethanol content in the fuels did not significantly impact the toxicity of EOM. Biological effects were mostly linked to xenobiotics metabolism and inflammatory response. BEAS-2B cells were more sensitive to the treatment.

1. Introduction

Health problems connected with air pollution caused by road traffic have been broadly studied for many years. The "traffic air" compounds are carbon oxides, polycyclic aromatic hydrocarbons (PAHs), nitrogen dioxide, particulate matter (PM), volatile organics, and heavy metals (reviewed by DeMarini, 2013). It has been proven that exposure to polluted air, mainly in large cities, increases the risk of diseases such as cancer and cardiovascular disorders, and also affects reproduction (reviewed by Lewtas, 2007). The International Agency for Research on Cancer confirmed the carcinogenetic role of diesel engine exhaust, and presumed the same for gasoline engine exhaust (IARC Monographs Diesel and gasoline engine exhausts and some nitroarenes, 2014). Yang et al. (Yang et al., 2019), showed that the toxic effects of gasoline engine exhaust are influenced by the ethanol content in the fuel blends. Some of the pollutants, such as acetaldehyde and formaldehyde, are contained at elevated concentrations in fuels with a higher ethanol percentage. On the contrary the proportions of hydrocarbons, PM, and gaseous toxins,

Abbreviations: 3D, Three dimensional; AK, Adenylate kinase; ALI, Air-liquid interface; ANOVA, Analysis of variance; BEAS-2B, Human bronchial epithelial cells; DNA, Deoxyribonucleic acid; dsDNA, Double-stranded deoxyribonucleic acid; E5, Ordinary gasoline, 5% ethanol blend; E20, Gasoline, 20% ethanol blend; ELISA, Enzyme-linked immunosorbent assay; ELLA, Sandwich enzyme-linked lectin assay; EOM, Extractable organic matter; gamma-H2AX, Phosphorylated histone H2AX; HPLC, High performance liquid chromatography; LDH, Lactate dehydrogenase; mRNA, Messenger ribonucleic acid; PAH, Polycyclic aromatic hydrocarbons; PM, Particulate matter; ROS, Reactive oxygen species; RT, Room temperature; T0, Time 0, before exposure; T1, Time after 1-day exposure; T5, Time after 5-day exposure.

* Corresponding author at: Department of Nanotoxicology and Molecular Epidemiology, Institute of Experimental Medicine CAS, Videnska 1083, 142 20 Prague, Czech Republic.

E-mail addresses: michal.sima@iem.cas.cz (M. Sima), tereza.cervena@iem.cas.cz (T. Cervena), fatima.elzeinova@iem.cas.cz (F. Elzeinova), antonin.ambroz@iem.cas.cz (A. Ambroz), vit.beranek@fs.cvut.cz (V. Beranek), michal.vojtisek@fs.cvut.cz (M. Vojtisek-Lom), klema@fel.cvut.cz (J. Klema), ciganek@vri.cz (M. Ciganek), pavel.rossner@iem.cas.cz (P. Rossner).

https://doi.org/10.1016/j.tiv.2022.105316
Received 25 June 2021; Received in revised form 13 December 2021; Accepted 14 January 2022
Available online 21 January 2022
0887-2333/© 2022 The Author(s). Published by Elsevier Ltd. This is an open access article under the CC BY-NC-ND license (http://creativecommons.org/licenses/by-nc-nd/4.0/).

are reduced with an increasing content of ethanol in the blends (Yang et al., 2019).

Due to ethical issues with human experimental exposures, along with the necessity to reduce animal experiments, new model systems had to be established. Owing to the imperfections of the most previously used cell monolayers (e.g. lacking of intra- and intercellular signaling, cancer cells with limited genetic stability), 3D (three dimensional) cell cultures have been developed. These usually contain cells of different types, and they can therefore simulate transcellular transport (Mercier et al., 2019), mucus barrier (reviewed by Ridley and Thornton, 2018), or tight junctions (Loiseau et al., 2020). For inhalation toxicology, where the effect of pollutants on cells in the lungs is most important, several models from this tissue have been developed (Balharry et al., 2008; Huang et al., 2017; Huang et al., 2013).

Mimicking real-world traffic exposure in in vitro experimental conditions can be performed in three ways: 1) by testing complete engine emissions (Cervena et al., 2021; Hawley et al., 2014; Mueller et al., 2010; Rossner et al., 2019), 2) by the application of extractable organic matter (EOM) from PM (Libalova et al., 2016, 2018a; Velali et al., 2016), or 3) by treatment with suspended particles (Gerlofs-Nijland et al., 2013; Ghio et al., 2013; Totlandsdal et al., 2015). All of these strategies have their own advantages but they also have limitations. When the system is exposed to complete emissions the most realistic representation of real-world conditions is achieved, but it can only be used for cells growing at the air-liquid interface (ALI) and not for submerged cultures. To reflect real-world scenarios, this experimental system also needs to take into account the air pollutant concentration changes over time (Good et al., 2016). Generally, 3D ALI studies with complete emissions have been limited to a short experimental duration lasting for several hours (Bisig et al., 2018; Bisig et al., 2016; Steiner et al., 2015; Steiner et al., 2012), although the results from 5-day exposure were also published (Cervena et al., 2021; Rossner et al., 2019). The exposure to organic extracts is only focused on soluble particles, while the effects of the gaseous pollutants are omitted. This leads to similar issues as with the exposure to suspended particles – the possible toxic effect of the other compounds is neglected, resulting in alterations of the pollutant-system interactions. However, the two latter techniques allow application of the simpler exposure design.

In this study we build upon our previous publications, where two cell models were exposed to complete emissions from a typical automobile direct injection gasoline (GDI) engine fueled with gasoline with 20% and 5% ethanol content, respectively (Cervena et al., 2021; Rossner et al., 2019). In these research papers, a comparison of short term (1-day) and long term (5-day) exposure of a commercial 3D model (MucilAir™, originating from bronchial epithelial tissue consisting of human basal, goblet, and ciliated cells) (Huang et al., 2013) and a typical monolayer culture (BEAS-2B), was performed for the emissions from each fuel individually. The presented results are from the exposure of MucilAir™ and BEAS-2B models to emissions from both the aforementioned fuels, specifically focusing on the biological effects of extractable organic matter from engine emission particles. Based on the cytotoxicity assays, mucin and extracellular reactive oxygen species production, DNA break detection and selected gene deregulation, we addressed the following questions: 1) are there any differences between short and long term exposure, 2) are there any differences between exposure to EOMs from fuels with a diverse ethanol content, 3) do the two cell models react variously, and 4) what are the differences in the toxicological effect of EOMs, compared to the complete emissions previously published (Cervena et al., 2021; Rossner et al., 2019)?

2. Material and methods

2.1. Cell cultures

BEAS-2B cell line, an immortalized non-tumorigenic human bronchial epithelial cell line, was purchased from ATCC (ATCC, Manassas, VA, USA). As previously described, BEAS-2B cell were seeded at 24-well Transwell® cell inserts (Sigma-Aldrich, St Louis, MO, USA) at a density of 100 000 cells/insert and kept in submerged conditions for 24 h. After that, apical medium was removed and the cells were kept at ALI conditions for 24 h prior to exposure (Cervena et al., 2021; Rossner et al., 2019). The cells were cultured at standard conditions (37 °C, 5% CO2, relative humidity >90%) using BEGM™ cell culture medium (CC-3170; Lonza, Basel, Switzerland).

The MucilAir™ human 3D culture (denoted as 3D model) inserts were purchased from Epithelix Sàrl (Geneva, Switzerland) and cultivated using a serum-free medium provided by the manufacturer (Epithelix Sàrl, Geneva, Switzerland). The manufacturer guaranteed uniform characteristics of the inserts, including comparable differentiation profiles. The inserts used in all the experiments consisted of bronchial epithelial cells, originating from a 64-year-old Caucasian female, non-smoker, with no pathology reported, a typical representative of a vulnerable population.

The medium was replaced every two to three days before exposure, and cell inserts were monitored under a light microscope (Olympus CKX41, Tokyo, Japan; 200× magnification).

2.2. Engine tests

A production direct injection spark ignition engine, designed to run on gasoline, and used in a popular EU passenger car, was used as the source of the emissions. To improve the stability of the emissions and to allow for accelerated cooling of the engine, allowing to run multiple cold start tests per day, the engine was mounted on a transient engine dynamometer and operated along speed-torque points observed on the same engine in a car during a World Harmonized Light Duty Vehicle Cycle (WLTC), a 30-min transient cycle covering urban, suburban, highway and motorway driving. A sample of the exhaust was taken immediately after the three-way catalyst and diluted in a partial flow dilution tunnel. Diluted exhaust was then routed to the air-liquid interface exposure system (see (Vojtisek-Lom et al., 2020), for details) and, in parallel, sampled onto fluorocarbon-coated borosilicate glass fiber filters (Pallflex TX40). A sequence consisting of cold start WLTC, hot start WLTC and two-hour pause during which the engine was actively cooled was repeated multiple times.

2.3. Exposure design

The exposure scheme was designed to match with previously carried out complete emission exposures (Cervena et al., 2021; Rossner et al., 2019). Filters with collected particulate matter were extracted with 60 mL of dichloromethane and 3 mL of cyclohexane for 3 h. The extracts obtained from the filters from each exposure experiment (i.e. 1-day and 5-day treatment) were pooled and a quantitative analysis of EOMs was executed by HPLC with fluorometric detection (PM mass and PAHs content in both EOMs and exposure doses are listed in Supplementary Table 1). EOMs were then evaporated under a stream of nitrogen and re-dissolved in dimethyl sulfoxide (DMSO) to a concentration of 100 μg/mL. The resulting solution was normalized per PM mass, but did not reflect particle numbers collected on individual filters. The exposure scheme consisted of 1 h incubation in culture medium, 1 h apical treatment with E5 or E20 EOMs or the negative control (15 L to a final concentration of 5 μg/mL selected as non-cytotoxic based on pilot experiments; data not shown), 2 h incubation in culture medium and a final 1 h incubation step (with 15 μL EOMs or the negative control). As the negative control, 0.1% DMSO in culture medium was used.

The cells/media were collected after the treatment and stored at −80 °C or − 20 °C for further analyses after 1-day (T1) or 5-day (T5) exposure. For 5-day exposures, the cells were provided with fresh medium and grown overnight. The following day, until day 5, the exposure commenced as described above. For each time point, samples from exposed and control cell cultures were obtained. For the purpose of this

study, exposure to EOM from an engine powered by E5 fuel, the marking is simplified to E5 exposure. A similar designation (E20 exposure) is used for exposure to EOM from an engine powered by E20 fuel.

2.4. Cytotoxicity assays

For the adenylate kinase activity detection, the cell culture medium was transferred into a white opaque 96 well plate, and then the AK Detection Reagent Working Solution was added (Abcam, Cambridge, UK). It was incubated for 5 min and subsequently the luminescence was read by SpectraMax®M5e (Molecular Devices, San Jose, CA, USA). The results were expressed as the percentage of cytotoxicity relative to the positive control (1% *v*/v Triton X-100, 1 h, and 37 °C).

The activity of lactate dehydrogenase (LDH) was analyzed in basal medium with the Cytotoxicity Detection Kit (Roche, Basel, Switzerland). The method was performed according to the manufacturer's instructions with some modifications: each sample was analyzed using 100 μL sample/well; 100 μL of the reaction mixture (Catalyst in H_2O + Dye solution) was added to each sample; the samples were incubated at RT on an orbital shaker in dark for 60 min. The absorbance was measured by SpectraMax®M5e (Molecular Devices, San Jose, CA, USA) at 490 nm. The final outcomes were expressed as the percentage of cytotoxicity relative to the positive control (1% v/v Triton X-100, 1 h, and 37 °C).

2.5. Mucin production quantification

For the quantification of mucin production, the sandwich enzyme-linked lectin assay (ELLA) developed by Epithelix Sàrl (Geneva, Switzerland) was used. This method relies on the interaction of lectins with mucin glycoproteins in apical wash. At each timepoint, 200 μL of apical wash was collected and the ELLA was conducted with modifications as reported in (Rossner et al., 2019).

2.6. Extracellular ROS production

ROS levels were measured in collected basal medium following the previously published protocol by Uy et al. (Uy et al., 2011). This simple method utilizes Acridan Lumigen PS-3 Assay (Pierce Biotechnology, Rockford, Illinois, USA) oxidation which generates luminescence. Briefly, 50 μL of Acridan Lumigen PS-3 assay solution was mixed with 100 μL of the collected medium and incubated in the dark for 5 min. Cell inserts cultivated with 250 μM hydrogen peroxide (H_2O_2) in the culture medium for 1 h at 37 °C were used as a positive control. All medium aliquots (including the positive control) were collected and stored at −20 °C prior to analysis. Luminescence was recorded with a SpectraMax® M5e spectrophotometer (integration time 500 ms).

2.7. Histone phosphorylation

In the inserts, cells were twice washed with PBS and lysed with 100 μl cold Lysis Buffer from the gamma-H2AX Pharmacodynamic Assay Kit (Trevigen. Gaithersburg, MD, USA). After 20 min incubation on ice the suspension was centrifuged. The protein concentration in the extracts was measured by the BCA Protein Assay (Sigma-Aldrich, St. Louis, MO, USA) and the extracts were then stored at −20 °C. For the gamma-H2AX assay, the samples were diluted to a concentration of 5 μg/well in the Assay Buffer, and after the ELISA procedure, the luminescence was measured by SpectraMax®M5e (Molecular Devices, San Jose, CA, USA).

2.8. mRNA expression analysis

After exposure (1-day/5-day), the cells from both cell lines were scraped and lysed in the inserts. The NucleoSpin RNA XS kit (Macherey-Nagel, Düren, Germany) was used for RNA isolation according to manufacturer's instructions. The concentration of extracted RNA was measured with the HS RNA kit by the Qubit 4 fluorometer (both Thermo Fisher Scientific, Wilmington, DE, USA) and the RNA integrity number was checked with the SS RNA kit by the Fragment Analyzer (both Agilent Technologies, Santa Clara, CA, USA).

RNA (400 ng) was used as the input for the targeted mRNA libraries construction, using the Human Molecular Toxicology Transcriptome panel with the QIAseq Targeted RNA 96-index HT for Illumina (both Qiagen, Hilden, Germany). With this panel, the expression of 370 genes was later detected (a list of the studied genes is presented in Supplementary Table 2). After the libraries were prepared, their concentration was measured with the 1× dsDNA HS kit (Thermo Fisher Scientific, Wilmington, DE, USA) on the Qubit 4 fluorometer, and their profile and size was analyzed by the Fragment Analyzer with the HS NGS Fragment Kit (Agilent Technologies, Santa Clara, CA, USA). For sequencing, the NextSeq system with the NextSeq 500/550 Mid Output Kit v2.5 (300 cycles) (both Illumina, San Diego, CA, USA) was utilized.

NF-CORE RNASeq pipeline (https://github.com/nf-core/rnaseq, version 1.3) (Ewels et al., 2020) was applied for RNA data processing as previously reported (Cervena et al., 2021; Rossner et al., 2019). The reference genome GRCh38.p12 was utilized for mapping the reads. DESeq2 with default parameter settings was used to normalize the read counts and to identify the differences in gene expression between the sample groups (Love et al., 2014). The Benjamini & Hochberg method was applied for multiple testing correction. All the genes located on chromosome X were omitted in the gene expression analyses, to account for the gender differences of subjects from which the MucilAir™ and BEAS-2B cells originated.

2.9. Statistical analysis

For all the analyses, the cells were exposed in biological triplicate. Furthermore, for cytotoxicity tests and gamma-H2AX phosphorylation detection, technical duplicates were used. The comparisons of parameters were performed by two-way ANOVA with Sidak's (post hoc) multiple comparison test and using Student's *t*-test (GraphPad Prism version 8 (GraphPad Software Inc., San Diego, CA, USA)). The results were expressed as mean ± standard deviation (SD). For AK, LDH, mucin, and extracellular ROS production, mean relative values were calculated as the ratio of averages of values after the exposure (T1 for 1-day exposure, T5 for 5-day exposure) and before exposures (T0). The Venn diagram for presenting common or unique gene deregulation was created by the Bioinformatics & Evolutionary Genomics tool (http://bioinformatics.psb.ugent.be/webtools/Venn/).

3. Results

3.1. Cytotoxicity detection

Cytotoxicity, assessed as the adenylate kinase and lactate dehydrogenase activities, was measured in the media of exposed cells and non-exposed controls, before and after the exposure of both cell lines to EOMs. In the following paragraphs, the cytotoxicity from experiments with values above 5% is reported as a relative value calculated as a ratio between post- and pre-exposure measurements. Averages and standard deviations of replicates with lower than 5% cytotoxicity values as well as the graphs with absolute cytotoxicity values from pre- and post-exposure measurements, are shown in Supplementary Table 3.

Overall, based on adenylate kinase activity, the cytotoxic effect of exposure to E5, as well as to E20 EOM was low. Values above 5% were only detected after the long exposure of BEAS-2B to both EOMs, and in the non-exposed samples. For both EOMs, the cytotoxicity was around 5% before the experiment and 10% after the exposure. In all time points, AK activity was significantly higher in the exposed than in non-exposed samples (Supplementary Table 3), and in post-exposure compared to the pre-exposure measurements (Fig. 1).

Similar, but more pronounced trends were observed when lactate dehydrogenase activity was detected. Values above 5% were found in

the media of both cell lines in the long exposure experiments to both EOMs. Higher mean relative values were noted for BEAS-2B cells than for MucilAir™, due to the higher pre-exposure values in this model. Both EOMs had similar effects on both cell models. After the 5-day measurements, the values were significantly higher than before exposure (Fig. 1, Supplementary Table 3).

3.2. Mucin production

A very low mucin concentration was detected in the insert apical washes of all the experiments with BEAS-2B. On the contrary, the highest values (around 10 μg/ml) were detected before the short exposure experiments with both fuels with MucilAir™ (Supplementary Table 3). In MucilAir™, a significant decrease between pre- and post-exposure in mucin production was detected after the 1-day experiment with E20 in the control samples, and after the 5-day experiment with E20 with the exposed and control samples. The significant changes in the controls suggest that the observed effects were related not only to EOM treatment, but also to the incubation conditions. The highest mean relative values were observed in the control samples after the 5-day experiment with E20. (Fig. 2).

3.3. Extracellular ROS

Significant differences in the extracellular ROS production (measured in the basal medium) between pre- and post-exposure were detected in MucilAir™ in the 1-day experiment with E20 (increased ROS levels), and in the 5-day experiment with both EOMs (decreased ROS production). In BEAS-2B cells, the post-exposure values significantly decreased when compared with the pre-exposure after the 1-day incubation with E5. After the long exposure experiments of BEAS-2B to both EOMs, no detectable values were found for the exposed and control samples (Fig. 3). No significant differences between the exposed and control samples were detected in both cell lines, EOMs, and all time points, indicating that the observed changes were related to the incubation conditions rather than to the effect of EOMs (Supplementary Table 3).

3.4. DNA break detection

Double-stranded DNA breaks were detected based on histone H2AX phosphorylation after both the short and long exposures in cell lysates. In all comparisons, there was a significant decrease in histone phosphorylation, when the long-exposed cells were compared to cells from the shorter exposure. A similar decrease was noted with both cell lines and both fuels, apart from MucilAir™ incubated with E20 where the reduction was less pronounced after the longer period. A significant difference between the exposed and control samples was observed after the long exposure of MucilAir™ to E5 (Fig. 4, Supplementary Table 3).

3.5. mRNA analysis

A differential expression analysis of a panel of 370 genes was performed after short (1-day) and long (5-day) exposure to EOMs. An overview of the number of up- and downregulated genes between individual exposure conditions is reported in Supplementary Table 4.

When gene expression in the exposed samples was compared with the controls, only *CYP1A1*, a gene encoding cytochrome P450 family 1 subfamily A member 1 protein, was differentially regulated. Upregulation of this gene expression was observed in all the exposure conditions for both EOMs. More pronounced changes were observed for MucilAir™ exposed to E5 EOM, particularly after the longer exposure time. On the contrary, for BEAS-2B cells there were greater changes detected after E20 exposure for the shorter time (Table 1).

After the simple exposed – non-exposed samples comparison, we looked for genes, whose expression differed between long and short exposure times. For this analysis, all differentially expressed genes in the control samples, or genes common for controls and exposed samples, were excluded to obtain only those specifically differing between exposure times. Such differentially expressed genes for E5 and E20 EOMs and genes specific for the control samples for selected comparisons between individual groups, are listed in Supplementary Table 5 and Supplementary Table 6, respectively.

While in MucilAir™ no significant differences were detected for E5 between 5-day and 1-day exposure, this EOM caused a differential expression of 13 genes in BEAS-2B cells. The expression of five and eight genes differed after exposure to E20 EOM in MucilAir™ or BEAS-2B cells, respectively, when the 5-day and 1-day treatment was

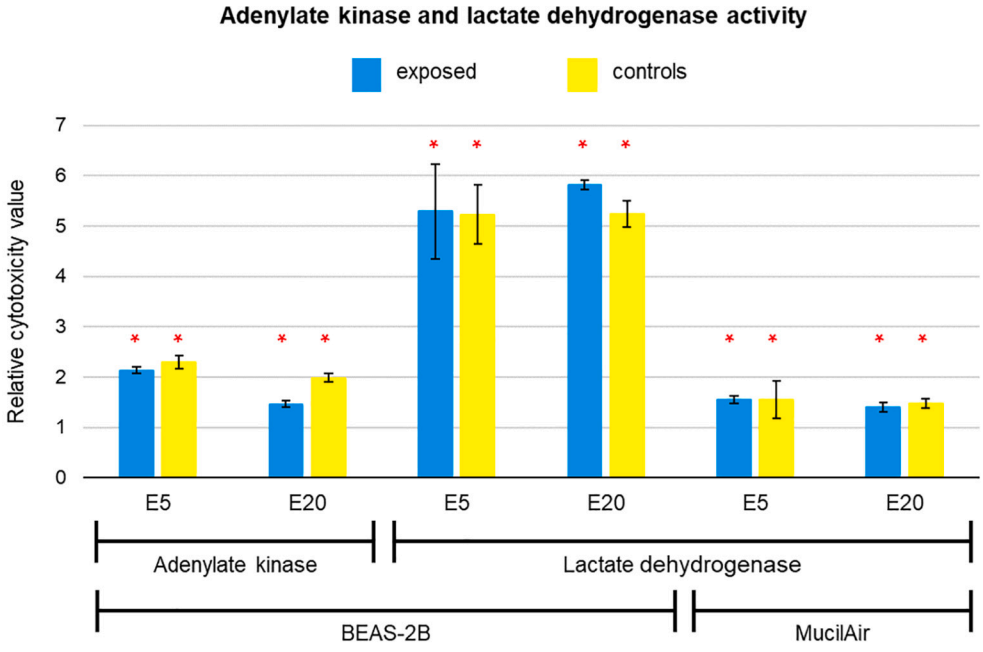

Fig. 1. Mean relative adenylate kinase and lactate dehydrogenase activity ± SD in media of two cell models exposed for 5 days to E5 and E20 EOMs or non-exposed controls. Blue columns (exposed) indicate the ratios between enzyme activities after- and before exposure to EOMs from E5 or E20, yellow columns (controls) denote the ratios between these values after and before 1- or 5-day experiments in which the cells were not exposed to EOMs. Asterisks denote significant differences when post-exposure samples were compared to pre-exposure samples ($p \leq 0.05$). Adenylate kinase activity in MucilAir™ as well as data from all 1-day exposures are not presented in this graph, as the values are below 5% (see Supplementary Table 3 for details). (For interpretation of the references to colour in this figure legend, the reader is referred to the web version of this article.)

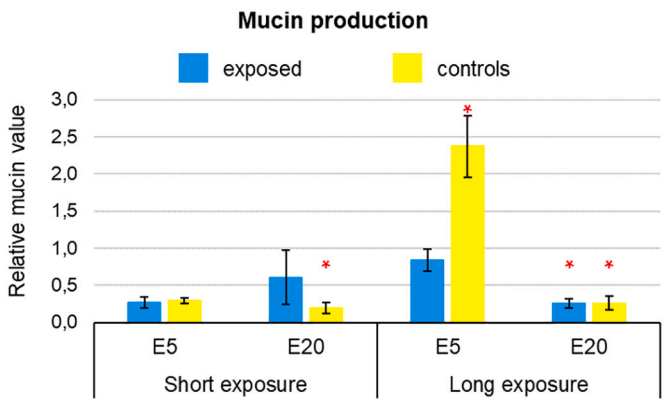

Fig. 2. Mean relative mucin production levels ± SD in MucilAir™ from the 1-(short) and 5-(long) day experiment with both EOMs. Blue columns (exposed) indicate the ratios between mucin production levels after- and before exposure to EOMs from E5 or E20, yellow columns (controls) denote the ratios between these values after and before 1- or 5-day experiments in which the cells were not exposed to EOMs. Asterisks denote significant differences when post-exposure samples were compared to pre-exposure samples ($p \leq 0.05$). Mucin production in BEAS-2B cells is not presented in this graph due to low values (See Supplementary Table 3 for details). (For interpretation of the references to colour in this figure legend, the reader is referred to the web version of this article.)

compared. Only two genes were commonly affected – one after BEAS-2B exposure to E5 and MucilAir™ to E20; and one after MucilAir™ and BEAS-2B cells exposure to E20 (Fig. 5).

Five genes differentially expressed in MucilAir™ after E20 EOM treatment were upregulated, indicating that their expression increases with prolonged exposure. Three out of these five genes are involved in immunotoxicity (tumor necrosis factor – *TNF*, interleukin 1 alpha – *IL1A*, and prostaglandin-endoperoxide synthase 2 – *PTGS2*). The remaining two (transgelin – *TAGLN* and TNF receptor superfamily member 10a – *TNFRSF10A*) play a role in phospholipidosis or apoptosis, respectively (Table 2).

In the comparison of 5-day and 1-day exposure of BEAS-2B to E5, seven genes were upregulated and six downregulated after the longer time. Flavin containing monooxygenase 2 and 4 (*FMO2* and *FMO4*) involved in cytochrome P450s and phase I drug metabolism pathways, were the two most upregulated in this analysis. The other five upregulated genes are connected to steatosis (peroxisome proliferator activated receptor alpha – *PPARA*, mitogen-activated protein kinase 8 – *MAPK8*, and propionyl-CoA carboxylase subunit alpha – *PCCA*), necrosis (Bcl2 modifying factor – *BMF*), or heat shock response (DnaJ heat shock protein family (Hsp40) member B1 – *DNAJB1*). The downregulation of six genes after 5-day exposure indicates the decreasing expression after longer treatment. These genes are involved in various pathways, such as mitochondrial energy metabolism, oxidative stress, and antioxidant response (uncoupling protein 3 – *UCP3*), immunotoxicity (interleukin 1 beta – *IL1B*, interleukin 1 alpha – *IL1A*), heat shock response (heat shock protein family E (Hsp10) member 1 – *HSPE1*), DNA damage and repair (ERCC excision repair 6, chromatin remodeling factor – *ERCC6*), or apoptosis (caspase 8 – *CASP8*) (Table 2).

In BEAS-2B cells exposed to E20, four genes were up- and four downregulated after the longer period when compared to the shorter one. The upregulated genes play a role in heat shock response (heat shock protein family A (Hsp70) member 9 – *HSPA9*), apoptosis (BCL2 apoptosis regulator – *BCL2*, Fas cell surface death receptor – *FAS*), and necrosis (HSPB1 associated protein 1 – *HSPBAP1*). Genes associated with apoptosis (TNF receptor superfamily member 10a – *TNFRSF10A*), oxidative stress and antioxidant response (peroxiredoxin 2 – *PRDX2*), fatty acid metabolism (acetyl-CoA acetyltransferase 2 – *ACAT2*), or mitochondrial energy metabolism (isocitrate dehydrogenase 3 (NAD (+)) beta – *IDH3B*) were downregulated (Table 2).

4. Discussion

The association between air pollution and human health is an intensively studied topic. Based on PubMed database, more than 32 thousand papers have investigated this link to date. One of the most important sources of pollution is traffic activity. This team have previously published several reports, where two cell models were exposed to complete emissions from fuels with 5% (E5) or 20% (E20) ethanol content (Cervena et al., 2021; Rossner et al., 2019). In this study, we focused on the effect of extractable organic matter from particulate matter collected from the emissions of these gasoline fuels. We performed cytotoxicity analyses, quantification of mucin and extracellular ROS production assessment, DNA breaks detection, and the analysis of the deregulation of selected genes. Based on these results, we investigated the influence of EOMs on two cell models after 1-day and 5-day exposure.

The cytotoxic effect of EOMs from both fuels was analyzed according to membrane damage detection by adenylate kinase and lactate dehydrogenase leakage. AK activity in MucilAir™ was negligible for short and long exposures to both EOMs. In BEAS-2B, the 5-day exposure induced significant cytotoxicity, with a slightly higher effect for E5. These observations were similar to the data obtained for complete E5 and E20 emissions in our previous studies (Cervena et al., 2021; Rossner et al., 2019).

The LDH activity after the short exposure to both EOMs was

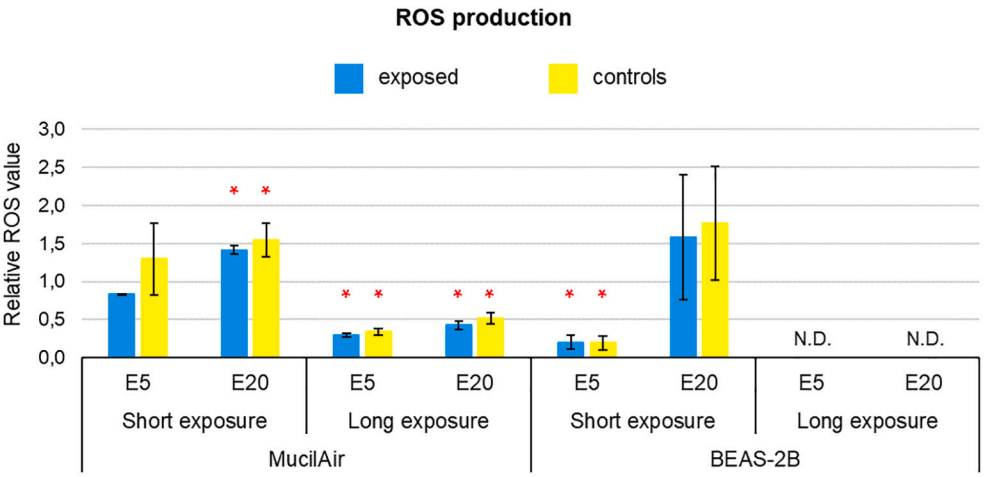

Fig. 3. Mean relative ROS production levels ± SD in MucilAir™ and BEAS-2B cell models in the short- and long-exposure experiments to E5 and E20. Blue columns (exposed) indicate the ratios between ROS production levels after- and before exposure to EOMs from E5 or E20, yellow columns (controls) denote the ratios between these values after and before 1- or 5-day experiments in which the cells were not exposed to EOMs. Asterisks denote significant differences when post-exposure samples were compared to pre-exposure samples ($p \leq 0.05$). (For interpretation of the references to colour in this figure legend, the reader is referred to the web version of this article.)

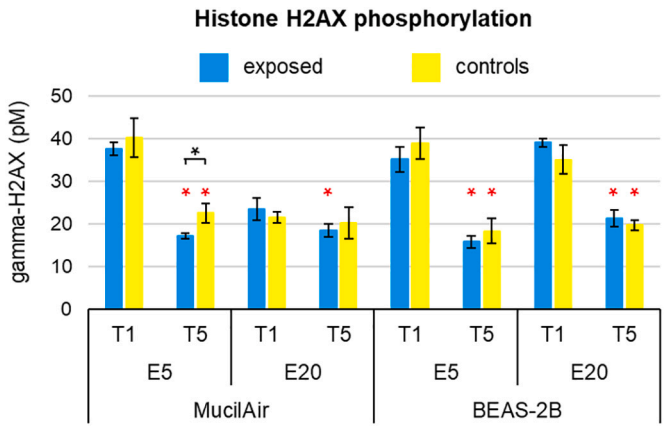

Fig. 4. Histone H2AX phosphorylation in MucilAir™ and BEAS-2B cells after the short- and long-exposure experiments to E5 and E20. Values after the short (T1) and the long (T5) experiment are indicated with standard deviations. Blue columns (exposed) indicate the ratios between histone H2AX phosphorylation after- and before exposure to EOMs from E5 or E20, yellow columns (controls) denote the ratios between these values after and before 1- or 5-day experiments in which the cells were not exposed to EOMs. Asterisks above brackets indicate significant difference between exposed and control samples. Red asterisks denote significant differences when samples after the long exposure were compared with samples after the short exposure (both $p \leq 0.05$). (For interpretation of the references to colour in this figure legend, the reader is referred to the web version of this article.)

Table 1
Deregulation of *CYP1A1* gene between exposed and control samples.

Cell line	Fuel	Exposure time	Log2 FC	Adjusted *p*-value
MucilAir™	E5	T1	4.815	2.02E-22
		T5	6.364	2.30E-39
	E20	T1	4.469	3.54E-19
		T5	5.948	2.74E-34
BEAS-2B	E5	T1	3.051	3.59E-07
		T5	2.497	2.01E-4
	E20	T1	3.686	7.46E-11
		T5	2.217	0.004

Differences in *CYP1A1* deregulation for MucilAir™/BEAS-2B cells, E5/E20 EOMs, and 1-day (T1)/5-day (T5) exposure time, when the exposed samples were compared with non-exposed controls. Log2 Fold Change and adjusted *p*-values are indicated for all comparisons

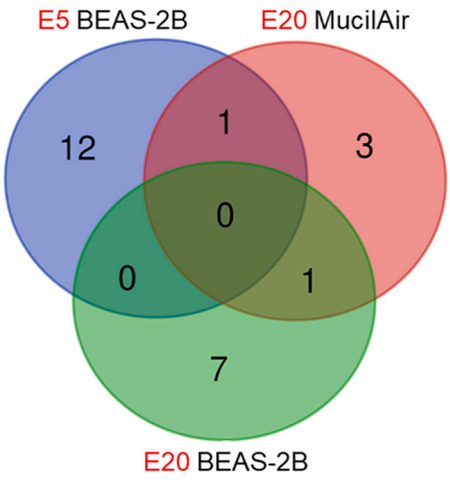

Fig. 5. Numbers of genes with specific deregulation when samples after 5-day exposure were compared with samples obtained from 1-day exposure. Common and unique deregulated genes in both cell lines and EOMs are indicated

generally very low. In contrast, after the long exposure, the LDH leakage was approximately twice as high compared to the AK activity, with greater post−/pre- exposure differences in BEAS-2B cells. Similarly, the impact of short exposure to complete emissions from E5 or E20 on these cell models was mostly low, while the 5-day exposure led to LDH activity reaching approximately 50% (Cervena et al., 2021; Rossner et al., 2019). In agreement with these papers, there were elevated levels of both cytotoxicity markers (mainly LDH) in the non-exposed controls after the treatment. This suggests, that measuring LDH activity could reflect not only the conditions related to exposure to the tested compounds, but also the processes which occur in connection with specific incubation requirements given by the experimental design.

It has been demonstrated, that mucins play a crucial role in protecting the lungs and airways against environmental pollutants, and their levels are increased when an organism reacts to inflammation (reviewed by (Ridley and Thornton, 2018). We have previously seen that exposure of BEAS-2B to complete emissions from E5 and E20 resulted in the elevation of mucin production, although the levels of mucin were very low at all time points for this cell line. On the contrary, the emissions caused a decrease of mucin levels in MucilAir™ (Cervena et al., 2021; Rossner et al., 2019). The trends for EOM exposure in the present study are similar: in BEAS-2B generally low mucin levels were detected and a decrease of mucin production was observed after MucilAir™ was exposed to both EOMs for 1 day and for 5 days to E20. In most of the experiments, non-significant differences were detected between the exposed and control samples. We assume, that changes in mucin levels after the exposure could be related to the protection of cells against the unfavorable conditions connected to the experimental design, and that a distinct reaction of MucilAir™ and BEAS-2B cells may be linked to the different adaptation abilities of these cells or a naturally higher production of mucin in MucilAir™.

The induction of ROS production and oxidative stress is usually caused by short exposure to various pollutants (reviewed by (Penning et al., 1999); (Baulig et al., 2009; Baulig et al., 2003; Murata et al., 2006; Shang et al., 2013; Tzeng et al., 2007). By contrast, in a recent study EOMs extracted from filters onto which air samples were collected in an industrial area, caused a decrease of ROS levels after longer exposure of two lung cell lines (A549 and HEL12469). The decrease was detected in all exposure conditions and was more pronounced in HEL12469 treated with higher EOMs concentration and for a longer exposure period (Libalova et al., 2018a). A similar pattern was found in our experiments. In most of the combinations, a significant decrease of extracellular ROS was observed after the exposure. The highest extracellular ROS levels were detected before the exposure of BEAS-2B cells (around 15%) whereas after the 5-day exposure, no detectable values were observed. Overall, lower ROS levels in MucilAir™ were found before exposure. All of these data indicate that the induction of ROS production by exposure to EOMs is time-dependent and is only observed after short exposures, which might be caused by the activation of an antioxidant response after the prolonged exposure.

The double-stranded DNA damage is frequently studied by the histone H2AX phosphorylation detection (reviewed by (Garcia-Canton et al., 2012). The genotoxic effect of organic compounds from particulate matter of various origin was previously reported (Audebert et al., 2010; Oya et al., 2011; Rossner et al., 2014; Toyooka et al., 2012). On the other hand, publications presented by our team on the exposure of MucilAir™ and BEAS-2B cells to complete gasoline engine emissions gave diverse results. While emissions from E20 fuel did not cause any increase of histone phosphorylation in MucilAir™, a significant induction of dsDNA damage was observed in BEAS-2B. In both cell models, longer exposure had a lower effect than the shorter one (Rossner et al., 2019). After the exposure of the cell models to emissions from E5 fuel, the only significant increase of histone phosphorylation was found after the 5-day treatment of MucilAir™. Moreover, a strong induction of dsDNA damage was detected in these cells when the long exposure was compared to the 1-day experiment (Cervena et al., 2021). In contrast,

Table 2
Gene deregulated after 5-days when compared with 1-day exposure.

EOM	Cell model	Ensemble ID	Gene Name	Log2 FC	Adjusted *p*-value	Biological pathways
E5	BEAS-2B	ENSG00000094963	*FMO2*	2.715	4.33E-06	Cytochrome P450s & Phase I Drug Metabolism
		ENSG00000076258	*FMO4*	0.970	0.007	Cytochrome P450s & Phase I Drug Metabolism
		ENSG00000186951	*PPARA*	0.787	0.001	Steatosis
		ENSG00000104081	*BMF*	0.632	0.030	Necrosis
		ENSG00000107643	*MAPK8*	0.529	0.031	Steatosis
		ENSG00000175198	*PCCA*	0.476	0.017	Steatosis
		ENSG00000132002	*DNAJB1*	0.302	0.045	Heat Shock Response
		ENSG00000064012	*CASP8*	−0.304	0.035	Apoptosis
		ENSG00000225830	*ERCC6*	−0.394	0.010	DNA Damage & Repair
		ENSG00000115541	*HSPE1*	−0.602	0.015	Heat Shock Response
		ENSG00000115008	*IL1A*	−0.805	0.010	Immunotoxicity
		ENSG00000125538	*IL1B*	−1.284	2.46E-04	Cholestasis & Immunotoxicity
		ENSG00000175564	*UCP3*	−1.955	0.029	Mitochondrial Energy Metabolism & Oxidative Stress & Antioxidant Response
E20	MucilAir™	ENSG00000232810	*TNF*	2.677	0.023	Apoptosis & Cholestasis & Immunotoxicity
		ENSG00000115008	*IL1A*	2.271	2.44E-04	Immunotoxicity
		ENSG00000149591	*TAGLN*	2.174	0.023	Phospholipidosis
		ENSG00000073756	*PTGS2*	1.022	0.023	Immunotoxicity
		ENSG00000104689	*TNFRSF10A*	0.671	0.031	Apoptosis
		ENSG00000113013	*HSPA9*	0.833	0.049	Heat Shock Response
	BEAS-2B	ENSG00000171791	*BCL2*	0.726	0.013	Apoptosis
		ENSG00000169087	*HSPBAP1*	0.586	0.012	Necrosis
		ENSG00000026103	*FAS*	0.354	0.037	Apoptosis & Steatosis & Immunotoxicity
		ENSG00000101365	*IDH3B*	−0.280	0.050	Mitochondrial Energy Metabolism
		ENSG00000120437	*ACAT2*	−0.347	0.039	Fatty Acid Metabolism
		ENSG00000167815	*PRDX2*	−0.470	0.036	Oxidative Stress & Antioxidant Response
		ENSG00000104689	*TNFRSF10A*	−0.487	0.036	Apoptosis

Specific gene deregulation for E5/E20 EOMs treatment of MucilAir™/BEAS-2B cells, when the 5-day exposure was compared with 1-day treatment, is listed in this table. Ensemble IDs, gene names, log2 FoldChange, adjusted p-values, and appropriate biological pathways are indicated for all comparisons. Genes in red or blue were commonly deregulated in more than one comparison

EOMs from these fuels did not show a significant increase of histone phosphorylation in the exposed samples. In nearly all of the 5-day experiments, the induction of dsDNA damage was significantly lower when compared to the shorter tests. Both EOMs had a similar effect on both cell lines. The distinct results obtained after exposure of MucilAir™/BEAS-2B cells to E5/E20 emissions/EOMs, suggest that each of these cell cultures may have diverse sensitivity and/or that the composition of the tested mixtures (namely particles and gaseous components of the exhaust) plays a role in DNA damage induction.

Finally, the detection of specific gene deregulation was performed in our study. The expression of 370 selected genes involved in biological pathways connected to the response to the toxic effects of engine exhaust was determined. Both EOMs had a similar impact on the expression of *CYP1A1* (cytochrome P450 family 1 subfamily A member 1). In all the studied comparisons, the exposure caused the up-regulation of this gene expression. While in MucilAir™, the longer exposure resulted in a stronger up-regulation of *CYP1A1* (mainly after E5 EOM treatment), the expression was more pronounced after the 1-day exposure in BEAS-2B. It was previously shown that this gene expression was deregulated after the exposure of MucilAir™ to benzo[*a*]pyrene, as well as to complete emissions from E5 and E20 fuels (Cervena et al., 2021; Cervena et al., 2019; Rossner et al., 2019). Our data are further supported by a study by (Libalova et al., 2018b), in which the expression of *CYP1A1* was induced after 24 h exposure of BEAS-2B to EOMs from neat gasoline fuel and from gasoline with 15% ethanol. The protein encoded by this gene is involved in the metabolism of PAHs, and the modulation of *CYP1A1* levels thus most likely reflects the response to these compounds present in tested EOMs.

We further searched for genes whose expression is exposure time-dependent. For this analysis, we compared expression levels after 5-day exposure with the shorter time interval. For EOMs from E5, we did not detect any significant differences between these periods in MucilAir™. On the contrary, a deregulation of 13 genes was observed for this comparison in BEAS-2B cells. Our results clearly showed that the expression of two genes (*FMO2* and *FMO4*) included in the cytochrome P450s and phase I drug metabolism pathways, increased in time. Diversely, the expression of genes connected with immunotoxicity or oxidative stress (*IL1A, IL1B,* and *UCP3*) was decreased. Interestingly, the deregulation of most of these genes was not detected after the exposure to complete emissions (Cervena et al., 2021; Rossner et al., 2019; Tomasek et al., 2018), suggesting an important role of organic components in modulation of the response. In studies investigating the effect of EOMs, a diverse response of proinflammatory cytokine expression was observed. In BEAS-2B cells, EOMs from various ethanol content gasoline fuels caused the downregulation of *IL1A* (Ahmed et al., 2020), while the expression of interleukins was upregulated after 24 h exposure of these cells to EOMs from other gasoline exhausts (Libalova et al., 2018b). It is generally accepted that inflammatory-related toxicity is mediated by particles and/or gaseous components of complete gasoline exhaust, as recently demonstrated for E5 emissions (Rossner et al., 2021). It is apparent, however, that organic compounds, such as PAHs, also modulate a pro-inflammatory response at certain conditions. As the previously mentioned studies did not contain the time dependent deregulation analysis, the modulation of gene expression detected in our study might suggest that it is time specific.

The expression of other genes was slightly different when the long and short exposure of BEAS-2B to E5 EOM was compared. It included genes involved in steatosis, heat shock response, apoptosis, or DNA damage. The expression changes of genes associated with these pathways were previously described after the exposure of cells exposed to complete emission from the E5 and E20 fuels (Cervena et al., 2021; Rossner et al., 2019), although the time-dependent effects were not investigated.

The exposure of MucilAir™ to E20 EOM increased the expression of five genes involved in apoptosis and immunotoxicity (including *IL1A*) when long and short treatments were compared. In BEAS-2B cells, the expression of eight genes differed between the exposure times. Similarly to MucilAir™, the genes associated with apoptosis and immunotoxicity were upregulated. The expression of four genes involved in other biological processes, such as mitochondrial energy metabolism, oxidative stress and antioxidant response, or apoptosis, was decreased after the long exposure, similarly as after the 5-day exposure to E5 EOM.

In this study, we detected deregulated genes after exposure to E20 EOM, for which no changes were observed in BEAS-2B cells exposed to complete E20 emissions (Rossner et al., 2019). In contrast, the emissions from E5 caused the deregulation of a higher number of genes than E5 EOM, mainly in the case of BEAS-2B cells (Cervena et al., 2021). More deregulated genes than after exposure to E5 or E20 EOMs were also detected, after BEAS-2B cells were exposed to EOMs from other gasoline fuels with various ethanol content (Ahmed et al., 2020; Libalova et al., 2018b).

Overall, the deregulation of genes involved in similar biological pathways was detected for both EOMs. Slight variations in response were probably caused by the different composition of EOMs. It was also speculated that each cell model might have the distinct ability to adapt to the exposure conditions, which could result in modulations of their reactions (Rossner et al., 2019). This hypothesis was also supported in our study by various deregulations of the same genes between cell models – upregulation of proinflammatory cytokine *IL1A* in MucilAir™ and downregulation in BEAS-2B. It was demonstrated, that the exposure of human nasal mucociliary airway epithelial cultures to EOM from PM of aerodynamic diameter 2.5 μm ($PM_{2.5}$) induced the expression of genes connected to mucus secretory program, as well as the expression of *CYP1A1* or *IL1A* (Montgomery et al., 2020). Considering the results of the present study, we assume this connection to be cell model specific. The upregulation of *CYPA1A* was detected after the exposure of both cell models to both EOMs for both exposure times, while the production of mucin decreased after exposure of MucilAir™ and was not detectable in BEAS-2B cells.

The different results observed for the analyzed endpoints for the tested cell models might be related to diverse character and properties of these cell cultures. BEAS-2B cells were established by transfection of bronchial epithelial cells by an adenovirus 12-SV40 hybrid virus and subsequent immortalization. They represent a typical cell culture consisting of a single cell type, standardly growing in the submerged conditions (Reddel et al., 1988). In contrast, MucilAir™ was obtained by reconstitution of human primary cells, consisting of several cell types (ciliated, mucus and basal cells) that remains fully differentiated while kept in the cell culture. It is further characterized by mucin production, cilia beating, established tight junctions, active ion transport, production of cytokines/chemokines, as well as the ability to grow at the air-liquid interface (Huang et al., 2013). Thus, our data might be regarded as a comparison of two different cell models, rather than a comparison of a 2D and a 3D culture. We assume that these differences that resulted in the fact that the cell models were not cultivated under identical conditions contributed to variability of the results.

In conclusion, we used extractable organic matter from particulate matter from E5 and E20 gasoline engine emissions to assess the toxic response in MucilAir™ and BEAS-2B cells after 1-day or 5-day exposure. Markers of toxicity, mucin and ROS production, double-stranded DNA damage, and the differential expression of selected genes were evaluated. As expected, most of our data show that the longer exposure had a greater effect on both cell models, as was also shown for the exposure to complete emissions (Cervena et al., 2021; Rossner et al., 2019). Only small differences were detected between EOMs from PM from fuels with distinct ethanol contribution, with BEAS-2B cells being more sensitive. These data also indicate a different response when compared with previously published information on the effect of complete emissions from the same fuels on the same cell cultures. The variations are most likely caused by differences in complete emissions/EOMs composition, but may be also related to specific exposure conditions used in our study, as suggested by significant changes of several endpoints in the control samples (e.g. mucin or extracellular ROS production). These parameters might not be optimal to evaluate EOMs toxicity in our experimental models, unless the impact of exposure is greater than variability detected in the control samples. Further, it should be pointed out that the results obtained for EOMs do not reflect biological impacts of engine emissions associated with real-world exposure, as they do not take into account the number of particles generated from individual fuels. They merely illustrate potential toxicity of organic extracts obtained from particles collected on the filters. Thus, our study should be regarded as a mechanistic investigation of impacts of EOM components, rather than a quantitative comparison of the tested fuels. Overall, choosing the correct cell model, type of the toxic compound, and exposure scheme, play a crucial role on the resulting data and all of these parameters should be taken into consideration when planning analogous experiments.

Supplementary data to this article can be found online at https://doi.org/10.1016/j.tiv.2022.105316.

Funding

This research was funded by the Czech Science Foundation (Project No. 18-04719S). The authors acknowledge the assistance provided by the Research Infrastructure NanoEnviCz, supported by the Ministry of Education, Youth and Sports of the Czech Republic under Project No. LM2018124 and the Research Infrastructure EATRIS-CZ, supported by the Ministry of Education, Youth and Sports of the Czech Republic under Project No. LM2018133. This work was supported by the Ministry of Education, Youth and Sports of the Czech Republic and The European Union - European Structural and Investments Funds in the frame of Operational Programme Research Development and Education - project Pro-NanoEnviCz (Project No. CZ.02.1.01/0.0/0.0/16_013/0001821).

Data availability statement

The data presented in this study are available in the Supplementary Materials.

Declaration of Competing Interest

The authors declare that they have no known competing financial interests or personal relationships that could have appeared to influence the work reported in this paper.

References

Ahmed, C.M.S., Yang, J., Chen, J.Y., Jiang, H., Cullen, C., Karavalakis, G., Lin, Y.-H., 2020. Toxicological responses in human airway epithelial cells (BEAS-2B) exposed to particulate matter emissions from gasoline fuels with varying aromatic and ethanol levels. Sci. Total Environ. 706, 135732 https://doi.org/10.1016/j.scitotenv.2019.135732.

Audebert, M., Riu, A., Jacques, C., Hillenweck, A., Jamin, E.L., Zalko, D., Cravedi, J.-P., 2010. Use of the gamma H2AX assay for assessing the genotoxicity of polycyclic aromatic hydrocarbons in human cell lines. Toxicol. Lett. 199, 182–192. https://doi.org/10.1016/j.toxlet.2010.08.022.

Balharry, D., Sexton, K., BeruBe, K.A., 2008. An in vitro approach to assess the toxicity of inhaled tobacco smoke components: nicotine, cadmium, formaldehyde and urethane. Toxicology 244, 66–76. https://doi.org/10.1016/j.tox.2007.11.001.

Baulig, A., Garlatti, M., Bonvallot, V., Marchand, A., Barouki, R., Marano, F., Baeza-Squiban, A., 2003. Involvement of reactive oxygen species in the metabolic pathways triggered by diesel exhaust particles in human airway epithelial cells. Am. J. Phys. Lung Cell. Mol. Phys. 285, L671–L679. https://doi.org/10.1152/ajplung.00419.2002.

Baulig, A., Singh, S., Marchand, A., Schins, R., Barouki, R., Garlatti, M., Marano, F., Baeza-Squiban, A., 2009. Role of Paris PM2.5 components in the pro-inflammatory response induced in airway epithelial cells. Toxicology 261, 126–135. https://doi.org/10.1016/j.tox.2009.05.007.

Bisig, C., Roth, M., Mueller, L., Comte, P., Heeb, N., Mayer, A., Czerwinski, J., Petri-Fink, A., Rothen-Rutishauser, B., 2016. Hazard identification of exhausts from gasoline-ethanol fuel blends using a multi-cellular human lung model. Environ. Res. 151, 789–796. https://doi.org/10.1016/j.envres.2016.09.010.

Bisig, C., Comte, P., Güdel, M., Czerwinski, J., Mayer, A., Müller, L., Petri-Fink, A., Rothen-Rutishauser, B., 2018. Assessment of lung cell toxicity of various gasoline engine exhausts using a versatile in vitro exposure system. Environ. Pollut. 235, 263–271. https://doi.org/10.1016/j.envpol.2017.12.061.

Cervena, T., Vrbova, K., Rossnerova, A., Topinka, J., Rossner, P., 2019. Short-term and long-term exposure of the MucilAir (TM) model to polycyclic aromatic hydrocarbons. Atla-Alternat. Lab. Anim. 47, 9–18. https://doi.org/10.1177/0261192919841484.

Cervena, T., Vojtisek-Lom, M., Vrbova, K., Ambroz, A., Novakova, Z., Elzeinova, F., Sima, M., Beranek, V., Pechout, M., Macoun, D., Klema, J., Rossnerova, A., Ciganek, M., Topinka, J., Rossner, P., 2021. Ordinary gasoline emissions induce a

toxic response in bronchial cells grown at air-liquid interface. Int. J. Mol. Sci. 22, 79. https://doi.org/10.3390/ijms22010079.
DeMarini, D.M., 2013. Genotoxicity biomarkers associated with exposure to traffic and near-road atmospheres: a review. Mutagenesis 28, 485–505. https://doi.org/10.1093/mutage/get042.
Diesel and gasoline engine exhausts and some nitroarenes, 2014. IARC Monographs on the Evaluation of Carcinogenic Risks to Humans.
Ewels, P.A., Peltzer, A., Fillinger, S., Patel, H., Alneberg, J., Wilm, A., Garcia, M.U., Di Tommaso, P., Nahnsen, S., 2020. The nf-core framework for community-curated bioinformatics pipelines. Nat. Biotechnol. 38, 276–278. https://doi.org/10.1038/s41587-020-0439-x.
Garcia-Canton, C., Anadon, A., Meredith, C., 2012. Gamma H2AX as a novel endpoint to detect DNA damage: applications for the assessment of the in vitro genotoxicity of cigarette smoke. Toxicol. in Vitro 26, 1075–1086. https://doi.org/10.1016/j.tiv.2012.06.006.
Gerlofs-Nijland, M.E., Totlandsdal, A.I., Tzamkiozis, T., Leseman, D.L.A.C., Samaras, Z., Lag, M., Schwarze, P., Ntziachristos, L., Cassee, F.R., 2013. Cell toxicity and oxidative potential of engine exhaust particles: impact of using particulate filter or biodiesel fuel blend. Environ. Sci. Technol. 47, 5931–5938. https://doi.org/10.1021/es305330y.
Ghio, A.J., Dailey, L.A., Soukup, J.M., Stonehuerner, J., Richards, J.H., Devlin, R.B., 2013. Growth of human bronchial epithelial cells at an air-liquid interface alters the response to particle exposure. Part. Fibre Toxicol. 10, 25. https://doi.org/10.1186/1743-8977-10-25.
Good, N., Molter, A., Ackerson, C., Bachand, A., Carpenter, T., Clark, M.L., Fedak, K.M., Kayne, A., Koehler, K., Moore, B., L'Orange, C., Quinn, C., Ugave, V., Stuart, A.L., Peel, J.L., Volckens, J., 2016. The Fort Collins commuter study: impact of route type and transport mode on personal exposure to multiple air pollutants. J. Exp. Sci. Environ. Epidemiol. 26, 397–404. https://doi.org/10.1038/jes.2015.68.
Hawley, B., L'Orange, C., Olsen, D.B., Marchese, A.J., Volckens, J., 2014. Oxidative stress and aromatic hydrocarbon response of human bronchial epithelial cells exposed to petro- or biodiesel exhaust treated with a diesel particulate filter. Toxicol. Sci. 141, 505–514. https://doi.org/10.1093/toxsci/kfu147.
Huang, S., Wiszniewski, L., Constant, S., Roggen, E., 2013. Potential of in vitro reconstituted 3D human airway epithelia (MucilAir (TM)) to assess respiratory sensitizers. Toxicol. in Vitro 27, 1151–1156. https://doi.org/10.1016/j.tiv.2012.10.010.
Huang, S., Boda, B., Vernaz, J., Ferreira, E., Wiszniewski, L., Constant, S., 2017. Establishment and characterization of an in vitro human small airway model (SmallAir (TM)). Eur. J. Pharm. Biopharm. 118, 68–72. https://doi.org/10.1016/j.ejpb.2016.12.006.
Lewtas, J., 2007. Air pollution combustion emissions: characterization of causative agents and mechanisms associated with cancer, reproductive, and cardiovascular effects. Mut. Res. Rev. Mut. Res. 636, 95–133. https://doi.org/10.1016/j.mrrev.2007.08.003.
Libalova, H., Rossner, P., Vrbova, K., Brzicova, T., Sikorova, J., Vojtisek-Lom, M., Beranek, V., Klema, J., Ciganek, M., Neca, J., Pencikova, K., Machala, M., Topinka, J., 2016. Comparative analysis of toxic responses of organic extracts from diesel and selected alternative fuels engine emissions in human lung BEAS-2B cells. Int. J. Mol. Sci. 17, 1833. https://doi.org/10.3390/ijms17111833.
Libalova, H., Milcova, A., Cervena, T., Vrbova, K., Rossnerova, A., Novakova, Z., Topinka, J., Rossner, P., 2018a. Kinetics of ROS generation induced by polycyclic aromatic hydrocarbons and organic extracts from ambient air particulate matter in model human lung cell lines. Mut. Res. Gen. Toxicol. Environ. Mutagen. 827, 50–58. https://doi.org/10.1016/j.mrgentox.2018.01.006.
Libalova, H., Rossner, P., Vrbova, K., Brzicova, T., Sikorova, J., Vojtisek-Lom, M., Beranek, V., Klema, J., Ciganek, M., Neca, J., Machala, M., Topinka, J., 2018b. Transcriptional response to organic compounds from diverse gasoline and biogasoline fuel emissions in human lung cells. Toxicol. in Vitro 48, 329–341. https://doi.org/10.1016/j.tiv.2018.02.002.
Loiseau, E., Gsell, S., Nommick, A., Jomard, C., Gras, D., Chanez, P., D'Ortona, U., Kodjabachian, L., Favier, J., Viallat, A., 2020. Active mucus-cilia hydrodynamic coupling drives self-organization of human bronchial epithelium. Nat. Phys. 16, 1158. https://doi.org/10.1038/s41567-020-0980-z.
Love, M.I., Huber, W., Anders, S., 2014. Moderated estimation of fold change and dispersion for RNA-seq data with DESeq2. Genome Biol. 15, 550. https://doi.org/10.1186/s13059-014-0550-8.
Mercier, C., Jacqueroux, E., He, Z., Hodin, S., Constant, S., Perek, N., Boudard, D., Delavenne, X., 2019. Pharmacological characterization of the 3D MucilAir (TM) nasal model. Eur. J. Pharm. Biopharm. 139, 186–196. https://doi.org/10.1016/j.ejpb.2019.04.002.
Montgomery, M.T., Sajuthi, S.P., Cho, S.-H., Everman, J.L., Rios, C.L., Goldfarbmuren, K. C., Jackson, N.D., Saef, B., Cromie, M., Eng, C., Medina, V., Elhawary, J.R., Oh, S.S., Rodriguez-Santana, J., Vladar, E.K., Burchard, E.G., Seibold, M.A., 2020. Genome-wide analysis reveals mucociliary remodeling of the nasal airway epithelium induced by urban PM(2.5). Am. J. Respir. Cell Mol. Biol. 63, 172–184. https://doi.org/10.1165/rcmb.2019-0454OC.
Mueller, L., Comte, P., Czerwinski, J., Kasper, M., Mayer, A.C.R., Gehr, P., Burtscher, H., Morin, J.-P., Konstandopoulos, A., Rothen-Rutishauser, B., 2010. New exposure system to evaluate the toxicity of (scooter) exhaust emissions in lung cells in vitro. Environ. Sci. Technol. 44, 2632–2638. https://doi.org/10.1021/es903146g.
Murata, M., Tezuka, T., Ohnishi, S., Takamura-Enya, T., Hisamatsu, Y., Kawanishi, S., 2006. Carcinogenic 3-nitrobenzanthrone induces oxidative damage to isolated and cellular DNA. Free Radic. Biol. Med. 40, 1242–1249. https://doi.org/10.1016/j.freeradbiomed.2005.11.015.
Oya, E., Ovrevik, J., Arlt, V.M., Nagy, E., Phillips, D.H., Holme, J.A., 2011. DNA damage and DNA damage response in human bronchial epithelial BEAS-2B cells following exposure to 2-nitrobenzanthrone and 3-nitrobenzanthrone: role in apoptosis. Mutagenesis 26, 697–708. https://doi.org/10.1093/mutage/ger035.
Penning, T.M., Burczynski, M.E., Hung, C.F., McCoull, K.D., Palackal, N.T., Tsuruda, L.S., 1999. Dihydrodiol dehydrogenases and polycyclic aromatic hydrocarbon activation: generation of reactive and redox active o-quinones. Chem. Res. Toxicol. 12, 1–18. https://doi.org/10.1021/tx980143n.
Reddel, R., Ke, Y., Gerwin, B., Mcmenamin, M., Lechner, J., Su, R., Brash, D., Park, J., Rhim, J., Harris, C., 1988. Transformation of human bronchial epithelial-cells by infection with sv40 or adenovirus-12 sv40 hybrid virus, or transfection via strontium phosphate coprecipitation with a plasmid containing sv40 early region genes. Cancer Res. 48, 1904–1909.
Ridley, C., Thornton, D.J., 2018. Mucins: the frontline defence of the lung. Biochem. Soc. Trans. 46, 1099–1106. https://doi.org/10.1042/BST20170402.
Rossner, P., Rossnerova, A., Beskid, O., Tabashidze, N., Libalova, H., Uhlirova, K., Topinka, J., Sram, R.J., 2014. Nonhomologous DNA end joining and chromosome aberrations in human embryonic lung fibroblasts treated with environmental pollutants. Mut. Res. Fund. Mol. Mech. Mutagen. 763, 28–38. https://doi.org/10.1016/j.mrfmmm.2014.03.006.
Rossner, P., Cervena, T., Vojtisek-Lom, M., Vrbova, K., Ambroz, A., Novakova, Z., Elzeinova, F., Margaryan, H., Beranek, V., Pechout, M., Macoun, D., Klema, J., Rossnerova, A., Ciganek, M., Topinka, J., 2019. The biological effects of complete gasoline engine emissions exposure in a 3D human airway model (MucilAir(TM)) and in human bronchial epithelial cells (BEAS-2B). Int. J. Mol. Sci. 20, 5710. https://doi.org/10.3390/ijms20225710.
Rossner, P., Cervena, T., Vojtisek-Lom, M., Neca, J., Ciganek, M., Vrbova, K., Ambroz, A., Novakova, Z., Elzeinova, F., Sima, M., Simova, Z., Holan, V., Beranek, V., Pechout, M., Macoun, D., Rossnerova, A., Topinka, J., 2021. Markers of lipid oxidation and inflammation in bronchial cells exposed to complete gasoline emissions and their organic extracts. Chemosphere 2021, 130833. https://doi.org/10.1016/j.chemosphere.2021.130833.
Shang, Y., Fan, L., Feng, J., Lv, S., Wu, M., Li, B., Zang, Y.-S., 2013. Genotoxic and inflammatory effects of organic extracts from traffic-related particulate matter in human lung epithelial A549 cells: the role of quinones. Toxicol. in Vitro 27, 922–931. https://doi.org/10.1016/j.tiv.2013.01.008.
Steiner, S., Mueller, L., Popovicheva, O.B., Raemy, D.O., Czerwinski, J., Comte, P., Mayer, A., Gehr, P., Rothen-Rutishauser, B., Clift, M.J.D., 2012. Cerium dioxide nanoparticles can interfere with the associated cellular mechanistic response to diesel exhaust exposure. Toxicol. Lett. 214, 218–225. https://doi.org/10.1016/j.toxlet.2012.08.026.
Steiner, S., Czerwinski, J., Comte, P., Heeb, N.V., Mayer, A., Petri-Fink, A., Rothen-Rutishauser, B., 2015. Effects of an iron-based fuel-borne catalyst and a diesel particle filter on exhaust toxicity in lung cells in vitro. Anal. Bioanal. Chem. 407, 5977–5986. https://doi.org/10.1007/s00216-014-7878-5.
Tomasek, I., Horwell, C.J., Bisig, C., Damby, D.E., Comte, P., Czerwinski, J., Petri-Fink, A., Clift, M.J.D., Drasler, B., Rothen-Rutishauser, B., 2018. Respiratory hazard assessment of combined exposure to complete gasoline exhaust and respirable volcanic ash in a multicellular human lung model at the air-liquid interface. Environ. Pollut. 238, 977–987. https://doi.org/10.1016/j.envpol.2018.01.115.
Totlandsdal, A.I., Lag, M., Lilleaas, E., Cassee, F., Schwarze, P., 2015. Differential Proinflammatory responses induced by diesel exhaust particles with contrasting PAH and metal content. Environ. Toxicol. 30, 188–196. https://doi.org/10.1002/tox.21884.
Toyooka, T., Shinmen, T., Aarts, J.M.M.J.G., Ibuki, Y., 2012. Dual effects of N-acetyl-l-cysteine dependent on NQO1 activity: suppressive or promotive of 9,10-phenanthrenequinone-induced toxicity. Toxicol. Appl. Pharmacol. 264, 404–412. https://doi.org/10.1016/j.taap.2012.08.017.
Tzeng, H.-P., Sen Yang, R., Ueng, T.-H., Liu, S.-H., 2007. Upregulation of cyclooxygenase-2 by motorcycle exhaust particulate-induced reactive oxygen species enhances rat vascular smooth muscle cell proliferation. Chem. Res. Toxicol. 20, 1170–1176. https://doi.org/10.1021/tx700084z.
Uy, B., McGlashan, S.R., Shaikh, S.B., 2011. Measurement of reactive oxygen species in the culture media using Acridan Lumigen PS-3 assay. J. Biomol. Tech. 22, 95–107.
Velali, E., Papachristou, E., Pantazaki, A., Choli-Papadopoulou, T., Argyrou, N., Tsourouktsoglou, T., Lialiaris, S., Constantinidis, A., Lykidis, D., Lialiaris, T.S., Besis, A., Voutsa, D., Samara, C., 2016. Cytotoxicity and genotoxicity induced in vitro by solvent-extractable organic matter of size-segregated urban particulate matter. Environ. Pollut. 218, 1350–1362. https://doi.org/10.1016/j.envpol.2016.09.001.
Vojtisek-Lom, Michal, Pechout, M., Macoun, D., Rameswaran, R., Praharaj, K.K., Cervena, T., Topinka, J., Rossner, P., 2020. Assessing exhaust toxicity with biological detector: configuration of portable air-liquid Interface human lung cell model exposure system. Sampling train and test conditions. SAE Int. J. Adv. & Curr. Prac. in Mobility 520–534. https://doi.org/10.4271/2019-24-0050.
Yang, J., Roth, P., Durbin, T.D., Shafer, M.M., Hemming, J., Antkiewicz, D.S., Asa-Awuku, A., Karavalakis, G., 2019. Emissions from a flex fuel GDI vehicle operating on ethanol fuels show marked contrasts in chemical, physical and toxicological characteristics as a function of ethanol content. Sci. Total Environ. 683, 749–761. https://doi.org/10.1016/j.scitotenv.2019.05.279.